



Synthesis of efficient blue phosphorescent heteroleptic Ir(III) complexes containing 4-alkoxy- or 4-alkylaminopicolinate as ancillary ligands



Hee Jung Choi^{a,b}, Myung Ho Hyun^{a,*}, Hea Jung Park^{a,*}, Ung Chan Yoon^{a,c,**}

^a Department of Chemistry and Chemistry Institute for Functional Materials, Pusan National University, Busan 46241, South Korea

^b Corporate R & D, LG Chem Ltd, Daejeon 34122, South Korea

^c ReSEAT, Korea Institute of Science and Technology Information (KISTI), Seoul 20456, South Korea

ARTICLE INFO

Keywords:

Phosphorescent Ir(III) complexes
Organic light emitting diode (OLED)
Blue-emitting
High phosphorescent quantum efficiency

ABSTRACT

New blue phosphorescent iridium(III) complexes containing 2-phenylpyridine derivatives as the main ligands and 4-substituted picolinate as the ancillary ligands were synthesized and their photophysical properties were investigated. In addition, the structures of three of the iridium(III) complexes were determined by X-ray crystallography. The photophysical data show that the introduction of electron-donating long-alkoxy or dialkylamino chain ($-\text{OCH}_2\text{CH}_2\text{OCH}_2\text{CH}_3$, $-\text{OC}_5\text{H}_{11}$, $-\text{OC}_6\text{H}_{13}$, $-\text{OC}_7\text{H}_{13}$, $-\text{N}(\text{C}_3\text{H}_7)_2$, or $-\text{N}(\text{C}_4\text{H}_9)_2$) on the 4-position of picolinate improved the phosphorescence quantum efficiencies ($\Phi_p = 0.57\text{--}0.77$) of synthesized iridium(III) complexes with the maximum emission range of 461–464 nm at 298 K in ethanol solution. Interestingly, the substitution of the methyl group at the 4-position of the pyridine ring of the 2-phenylpyridine main ligands in the complexes with a more strongly electron-donating methoxy or dimethylamino group results in a significant bathochromic shift (69 nm) rather than a hypsochromic shift of the phosphorescence emission maxima. Density field theory (DFT) calculations were performed to gain deeper understanding of these emission behaviors. The thermally most stable **Ir7** among the synthesized blue phosphorescent iridium(III) complexes was tested as an emitting material in a simple OLED device.

1. Introduction

Development of highly efficient OLEDs using phosphorescent materials have been investigated persistently [1–16]. Among the OLEDs containing heavy metal complexes, those with iridium(III) as the metal center were found to display the best performance in terms of the high photoluminescence (PL) efficiencies and relatively short excited state lifetimes, which minimizes the quenching of the triplet emissive states [17]. There have been intense studies to improve the OLED performances in a device structure aspect [18–27]. However, fundamental study to develop highly efficient blue phosphorescent materials is essential to embody perfect color in display applications.

Earlier studies showed that the homoleptic iridium(III) complex, tris-(2-phenylpyridinato-N,C^{2'})iridium(III), Ir(ppy)₃, has a LUMO that is localized mainly on the pyridine ring of the 2-phenylpyridine moiety whereas its HOMO is largely localized on the phenyl ring of this ligand [28,29]. Moreover, electron-donating group substitution on the C-4 position of the pyridine ring of the ligand causes an increase in the LUMO energy, and electron-withdrawing group substitution on the phenyl ring of the ligand lowers the HOMO energy. As a result, a

combination of these substitution patterns leads to a larger band gap between the HOMO and LUMO levels, and consequently, a hypsochromic (blue) shift of emission. Therefore, it is possible to propose a pattern for substitutions on the ligand of this homoleptic complex that leads to optimized blue phosphorescent iridium complexes, as depicted in Fig. 1(a).

In accordance with the proposal, Thompson reported that the heteroleptic iridium(III) bis[(4,6-di-fluorophenyl)-pyridinato-N,C^{2'}]picolinate (FIrpic) (Fig. 1(b)), which contains two electron-withdrawing fluorine groups on the phenyl ring of the main ligand and a new picolinate as the ancillary ligand, emits blue phosphorescence [30,31]. A comparison of the structure of heteroleptic FIrpic with those of the ideal homoleptic blue phosphorescent iridium complexes shown in Fig. 1(a) led to the development of a new strategy for the design of blue phosphorescent iridium complexes containing 4-substituted picolinate ancillary ligands. The carboxylate group of the picolinate ancillary ligands in the heteroleptic complexes serves as an electron withdrawing substituent on the pyridine ring of the ancillary ligand. Therefore, the picolinate can be considered as a surrogate for an electron-withdrawing group substituted, electron-deficient phenyl ring (2-phenylpyridine

* Corresponding authors.

** Corresponding author at: ReSEAT, Korea Institute of Science and Technology Information (KISTI), Seoul 20456, South Korea.

E-mail addresses: mhyun@pusan.ac.kr (M.H. Hyun), heajungp@pusan.ac.kr (H.J. Park), ucyoon@pusan.ac.kr (U.C. Yoon).

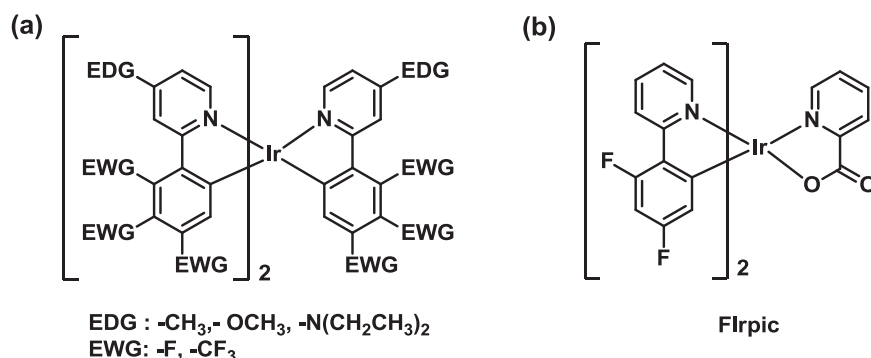


Fig. 1. (a) Structural patterns of the blue phosphorescent homoleptic iridium(III) complexes and (b) Firpic, heteroleptic iridium(III) complex containing the picolinate ancillary ligand.

moiety) (Fig. 1(a)) required to create a large HOMO/LUMO energy gap, resulting in blue phosphorescence. Furthermore, it was assumed that the emission wavelengths of the complexes can be tuned by varying the electronic properties of the substituents at the C-4 of the picolinate ancillary ligand. Accordingly, it was predicted that the introduction of electron-donating groups at this position would lead to an increase in the LUMO energy and a hypsochromic shift in emission.

Recently we initiated a program aimed at developing new blue phosphorescent heteroleptic iridium(III) complexes (Fig. 2), employing a design strategy that is based on the selection of properly substituted 2-phenylpyridines as main ligands and picolinates as ancillary ligands. The rationally designed, main ligands explored in this effort include 2-(2',4'-difluorophenyl)-4-methyl-, 2-(2',4'-difluorophenyl)-4-methoxy-, 2-(2',4'-difluorophenyl)-4-(dimethylamino)-, and 2-(2',5'-difluorophenyl)-4-methyl-pyridine and ancillary ligands include 4-alkoxy-pyridines, and 4-(dimethylamino)pyridine. To probe the validity of this strategy and the supporting assumptions, electron-withdrawing fluoro groups are introduced at the 2-, 4- or 5-positions of the phenyl ring of the main ligands. The complexes were synthesized and their photophysical and electrochemical properties were characterized. Finally, OLED devices containing complexes, which were found to have optimal blue emission properties, were constructed and tested. The results of this effort are described and discussed below.

2. Experimental

All reagents were obtained from commercial sources and used as received and the solvents were dried by using standard procedures. Main ligands, 2-(2',4'-difluorophenyl)pyridine, 2-(2',4'-difluorophenyl)-4-methylpyridine, 2-(2',4'-difluorophenyl)-4-dimethylaminopyridine, and 2-(2',5'-difluorophenyl)-4-methylpyridine were prepared by following literatures [32,33]. Heteroleptic iridium(III) complexes, **Ir1–Ir10**, were prepared via their corresponding μ -chloro-bridged dimers. Detailed synthetic procedures are described in supplementary information.

The ^1H - (300 MHz) and ^{13}C NMR (75 MHz) spectra were recorded using CDCl_3 solutions and the chemical shifts are reported as parts per million relative to CHCl_3 (7.26 ppm for ^1H NMR and 77.0 ppm for ^{13}C NMR) as an internal standard. The reactions were monitored by thin layer chromatography (TLC). Commercial TLC plates (Silica gel 60 F_{254} , Merck Co.) were developed and the spots were observed under UV light at a short wavelength of 254 nm and long wavelength of 365 nm. The

high-resolution mass spectral data were obtained at the Korea Basic Science Institute Daegu Center (HR-FAB Mass) on a Jeol JMS 700 high resolution mass spectrometer and at Daejeon Center (HR-ESI Mass).

2.1. Typical method

$\text{C}^*\text{N}_2\text{Ir}(\mu\text{-Cl})_2\text{IrC}^*\text{N}_2$ [$\text{C}^*\text{N} = 2$ -(2',4'-difluoro-phenyl)-4-methylpyridine] complex (**10**) (0.07 g, 0.06 mmol), 4-chloropicolinic acid (**15**) (0.02 g, 0.15 mmol) and sodium carbonate (0.1 g, 0.9 mmol) were placed in a 50 mL one-necked round bottom flask equipped with a condenser. The flask was evacuated and filled with Ar gas three times. 2-Ethoxyethanol (**16**) (12 mL) was then added. In this reaction, solvent, 2-ethoxyethanol (**16**) acted as a nucleophile. The mixture was stirred under reflux for 24 h in an Ar atmosphere and cooled to room temperature. 2-Ethoxyethanol was removed by rotary evaporation. The residue was dissolved in water and extracted with CH_2Cl_2 . The combined organic layers were washed with brine, dried over Na_2SO_4 and concentrated using a rotary evaporator. The light yellow residue was subjected to chromatography over silica gel. Additional purification was carried out by recrystallization (dichloromethane/ n-hexane) to provide **Ir2** (0.07 g, 68%) as a light yellow crystals. Iridium(III) complexes **Ir3–Ir10** were prepared from the corresponding commercially available alcohols or amines, **28–33**, as nucleophiles by using a similar procedure.

Iridium(III) bis(2-(2',4'-difluorophenyl)-4-methylpyridinato- N,C^2) 4-(2'-(ethoxy)ethoxy)picolinate (Ir2, 68%): ^1H NMR (CDCl_3) δ 1.22 (t, $J = 6.9$ Hz, 3 H), 2.54 (s, 6 H), 3.53 (dd, $J = 14.1, 6.9$ Hz, 2 H), 3.80 (t, $J = 4.4$ Hz, 2 H), 4.22 (dd, $J = 7.4, 4.2$ Hz, 2 H), 5.58 (dd, $J = 8.7, 2.1$ Hz, 1 H), 5.79 (dd, $J = 8.7, 2.1$ Hz, 1 H), 6.36–6.44 (m, 2 H), 6.78 (dd, $J = 5.7, 0.9$ Hz, 1 H), 6.91 (dd, $J = 6.0, 2.7$ Hz, 1 H), 6.98 (dd, $J = 5.7, 0.9$ Hz, 1 H), 7.27 (d, $J = 5.7$ Hz, 1 H), 7.48 (d, $J = 6.3$ Hz, 1 H), 7.82 (d, $J = 2.7$ Hz, 1 H), 8.02 (bs, 1 H) 8.09 (bs, 1 H), 8.51 (d, $J = 6.0$ Hz, 1 H). HRMS (ESI) $[\text{M} + \text{H}]^+$, Calcd for $\text{C}_{34}\text{H}_{29}\text{F}_4\text{IrN}_3\text{O}_4$ 812.1719, found 812.1725. Anal. Calcd for $\text{C}_{34}\text{H}_{28}\text{F}_4\text{IrN}_3\text{O}_4$: C, 50.36; H, 3.48; N, 5.18. Found: C, 48.75; H, 3.08; N, 5.08.

Iridium(III) bis(2-(2',4'-difluorophenyl)-4-methylpyridinato- N,C^2) 4-(pentyloxy)picolinate (Ir3, 60%): ^1H NMR (CDCl_3) δ 0.90 (t, $J = 7.1$ Hz, 3 H), 1.32–1.44 (m, 4 H), 1.74–1.83 (m, 2 H), 2.52 (s, 6 H), 4.08 (t, $J = 6.6$ Hz, 2 H), 5.58 (dd, $J = 9.0, 2.4$ Hz, 1 H), 5.80 (dd, $J = 9.0, 2.4$ Hz, 1 H), 6.31–6.46 (m, 2 H), 6.77 (dd, $J = 6.0, 1.8$ Hz, 1 H), 6.81 (dd, $J = 6.3, 2.7$ Hz, 1 H), 6.97 (dd, $J = 5.7, 1.2$ Hz, 1 H), 7.31 (d, $J = 6.3$ Hz, 1 H), 7.46 (d, $J = 6.3$ Hz, 1 H), 7.79 (d, $J = 2.7$ Hz, 1 H), 8.02

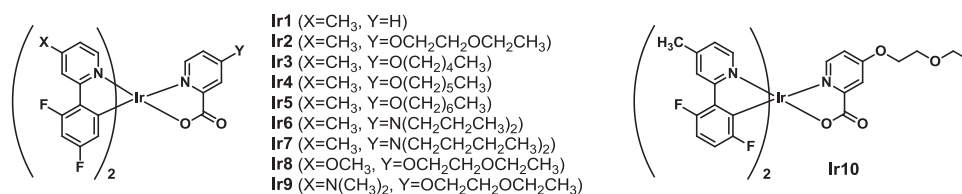


Fig. 2. Molecular structures of iridium(III) complexes, **Ir1–Ir10**.

(bs, 1 H), 8.08 (bs, 1 H), 8.52 (dd, $J=6.0$ Hz, 1 H). HRMS (ESI) $[M+H]^+$, Calcd for $C_{35}H_{31}F_4IrN_3O_3$ 810.1927, found 810.1937. Anal. Calcd for $C_{35}H_{30}F_4IrN_3O_3$: C, 51.97; H, 3.74; N, 5.20. Found: C, 48.68; H, 2.58; N, 4.58.

Iridium(III) bis(2-(2',4'-difluorophenyl)-4-methylpyridinato- N,C^2) 4-(hexyloxy)picolinate (Ir4, 57%): 1H NMR ($CDCl_3$) δ 0.88 (t, $J=6.6$ Hz, 3 H), 1.24–1.31 (m, 4 H), 1.35–1.42 (m, 2 H), 1.72–1.81 (m, 2H), 2.51 (s, 6 H), 4.06 (t, $J=1.2$ Hz, 2 H), 5.60 (dd, $J=9.0$, 2.4 Hz, 1 H), 5.79 (dd, $J=9.0$, 2.4 Hz, 1 H), 6.30–6.45 (m, 2 H), 6.77 (dd, $J=6.0$, 1.2 Hz, 1 H), 6.81 (dd, $J=6.3$, 3.0 Hz, 1 H), 6.97 (dd, $J=6.0$, 1.2 Hz, 1 H), 7.31 (d, $J=5.7$ Hz, 1 H), 7.46 (d, $J=6.0$ Hz, 1 H), 7.78 (d, $J=2.7$ Hz, 1 H), 8.01 (bs, 1 H), 8.07 (bs, 1 H), 8.52 (dd, $J=6.0$ Hz, 1 H). HRMS (ESI) $[M+H]^+$, Calcd for $C_{36}H_{33}F_4IrN_3O_3$ 824.2083, found 824.2072. Anal. Calcd for $C_{36}H_{32}F_4IrN_3O_3$: C, 52.55; H, 3.92; N, 5.11. Found: C, 50.40; H, 2.69; N, 4.53.

Iridium(III) bis(2-(2',4'-difluorophenyl)-4-methylpyridinato- N,C^2) 4-(heptyloxy)picolinate (Ir5, 43%): 1H NMR ($CDCl_3$) δ 0.88 (t, $J=4.5$ Hz, 3 H), 1.25–1.44 (m, 8 H), 1.74–1.83 (m, 2 H), 2.53 (s, 6 H), 4.08 (t, $J=6.3$ Hz, 2 H), 5.58 (dd, $J=9.0$, 2.4 Hz, 1 H), 5.80 (dd, $J=9.0$, 2.4 Hz, 1 H), 6.32–6.47 (m, 2 H), 6.78 (d, $J=5.7$ Hz, 1 H), 6.99 (d, $J=6.0$ Hz, 1 H), 7.31 (d, $J=6.3$ Hz, 1 H), 7.47 (d, $J=5.7$ Hz, 1 H), 7.80 (d, $J=2.7$ Hz, 1 H), 8.02 (bs, 1H), 8.09 (bs, 1 H), 8.55 (dd, $J=6.0$ Hz, 1 H). HRMS (ESI) $[M+H]^+$, Calcd for $C_{37}H_{35}F_4IrN_3O_3$ 838.2239, found 838.2247. Anal. Calcd for $C_{37}H_{34}F_4IrN_3O_3$: C, 53.10; H, 4.09; N, 5.02. Found: C, 52.62; H, 3.32; N, 4.98.

Iridium(III) bis(2-(2',4'-difluorophenyl)-4-methylpyridinato- N,C^2) 4-(dipropylamino)picolinate (Ir6, 70%): 1H NMR ($CDCl_3$) δ 0.91 (t, $J=7.2$ Hz, 6 H), 1.53–1.66 (m, 4 H), 2.53 (d, $J=3.9$ Hz, 6 H), 3.27 (dd, $J=9.0$, 6.3 Hz, 4 H), 5.61 (dd, $J=8.7$, 2.1 Hz, 1 H), 5.82 (dd, $J=8.7$, 2.1 Hz, 1 H), 6.29–6.43 (m, 3 H), 6.80 (d, $J=5.7$ Hz, 1 H), 6.98 (d, $J=6.0$ Hz, 1 H), 7.18 (d, $J=6.6$ Hz, 1 H), 7.44 (d, $J=8.1$ Hz, 1 H), 7.45 (s, 1 H), 8.01 (s, 1 H), 8.07 (s, 1 H), 8.72 (d, $J=5.7$ Hz, 1 H). HRMS (ESI) $[M+H]^+$, Calcd for $C_{36}H_{34}F_4IrN_4O_2$ 823.2244, found 823.2242. Anal. Calcd for $C_{36}H_{33}F_4IrN_4O_2$: C, 52.61; H, 4.05; N, 6.82. Found: C, 52.52; H, 3.75; N, 6.28.

Iridium(III) bis(2-(2',4'-difluorophenyl)-4-methylpyridinato- N,C^2) 4-(dibutylamino)picolinate (Ir7, 70%): 1H NMR ($CDCl_3$) δ 0.94 (t, $J=7.5$ Hz, 6 H), 1.25–1.37 (m, 4 H), 1.53–1.58 (m, 4 H), 2.53 (d, $J=3.0$ Hz, 6 H), 3.27 (dd, $J=8.7$, 5.7 Hz, 4 H), 5.59 (dd, $J=8.7$, 2.1 Hz, 1 H), 5.80 (dd, $J=9.0$, 2.7 Hz, 1 H), 6.29–6.44 (m, 3 H), 6.80 (dd, $J=6.0$, 1.2 Hz, 1 H), 7.00 (dd, $J=6.0$, 1.2 Hz, 1 H), 7.17 (d, $J=6.0$ Hz, 1 H), 7.43 (dd, $J=5.4$, 3.0 Hz, 2 H), 8.02 (bs, 1 H), 8.07 (bs, 1 H), 8.56 (d, $J=6.0$ Hz, 1 H). HRMS (ESI) $[M+H]^+$, Calcd for $C_{38}H_{38}F_4IrN_4O_2$ 851.2553, found 851.2556. Anal. Calcd for $C_{38}H_{37}F_4IrN_4O_2$: C, 53.70; H, 4.39; N, 6.59. Found: C, 53.51; H, 4.29; N, 6.60.

Iridium(III) bis(2-(2',4'-difluorophenyl)-4-methoxy)pyridinato- N,C^2) 4-(2'-(ethoxy)ethoxy)picolinate (Ir8, 50%): 1H NMR ($CDCl_3$) δ 1.22 (t, $J=6.9$ Hz, 3 H), 3.57 (q, $J=7.0$ Hz, 2 H), 3.79 (t, $J=4.1$ Hz, 2 H), 4.25 (q, $J=3.6$ Hz, 2 H), 5.66 (dd, $J=8.7$, 2.1 Hz, 1 H), 5.85 (dd, $J=8.7$, 2.4 Hz, 1 H), 6.32–6.47 (m, 2 H), 6.54 (dd, $J=6.5$, 2.4 Hz, 1 H), 6.74 (dd, $J=6.6$, 2.7 Hz, 1 H), 6.92 (dd, $J=6.2$, 2.7 Hz, 1 H), 7.22 (d, $J=6.3$ Hz, 1 H), 7.50 (d, $J=6.0$ Hz, 1 H), 7.71 (dd, $J=2.7$, 2.7 Hz, 1 H), 7.77 (dd, $J=3.2$, 3.2 Hz, 1 H), 7.83 (d, $J=2.7$ Hz, 1 H), 8.47 (d, $J=6.6$ Hz, 1 H). HRMS (ESI) $[M+H]^+$, Calcd for $C_{34}H_{29}F_4IrN_3O_6$ 844.1625, found 844.1616. Anal. Calcd for $C_{34}H_{28}F_4IrN_3O_6$: C, 48.45; H, 3.35; N, 4.99. Found: C, 47.39; H, 3.82; N, 4.74.

Iridium(III) bis(2-(2',4'-difluorophenyl)-4-(dimethylamino)pyridinato- N,C^2) 4-(2'-(ethoxy)ethoxy)picolinate (Ir9, 51%): 1H NMR ($CDCl_3$) δ 1.22 (t, $J=7.1$ Hz, 3 H), 3.13 (d, $J=2.7$ Hz, 12 H), 3.57 (q, $J=6.9$ Hz, 2 H), 3.79 (t, $J=3.6$ Hz, 2 H), 4.24 (q, $J=3.6$ Hz, 2 H), 5.76 (dd, $J=8.9$, 2.7 Hz, 1 H), 5.92 (dd, $J=9.0$, 2.4 Hz, 1 H), 6.18 (dd, $J=5.3$, 2.7 Hz, 1 H), 6.28–6.43 (m, 3H), 6.89 (dd, $J=6.3$, 2.7 Hz, 1 H), 6.97 (d, $J=6.6$ Hz, 1 H), 7.39 (dd, $J=3.2$, 3.2 Hz, 1 H), 7.46 (dd, $J=3.5$, 3.5 Hz, 1 H), 7.84 (d, $J=3.0$ Hz, 1 H), 8.15 (d, $J=6.9$ Hz, 1 H). HRMS (ESI) $[M+H]^+$, Calcd for $C_{36}H_{34}F_4IrN_4O_2$ 870.2250, found

870.2249. Anal. Calcd for $C_{36}H_{33}F_4IrN_4O_2$: C, 52.61; H, 4.05; N, 6.82. Found: C, 49.64; H, 4.21; N, 7.07.

Iridium(III) bis(2-(2',5'-difluorophenyl)-4-methylpyridinato- N,C^2) 4-(2'-(ethoxy)ethoxy)picolinate (Ir10, 70%): 1H NMR ($CDCl_3$) δ 1.22 (t, $J=6.9$ Hz, 3 H), 2.49 (d, $J=1.8$ Hz, 6 H), 3.57 (q, $J=7.1$ Hz, 2 H), 3.77 (t, $J=4.2$ Hz, 2 H), 4.24 (q, $J=4.2$ Hz, 2 H), 6.30–6.46 (m, 2 H), 6.52–6.68 (m, 2 H), 6.72 (d, $J=4.8$ Hz), 6.91 (d, $J=6.0$ Hz, 1 H), 7.28 (d, $J=6.0$ Hz, 1 H), 7.53 (d, $J=6.0$ Hz, 1 H), 7.81 (d, $J=2.7$ Hz, 1 H), 8.06 (bs, 1 H), 8.14 (bs, 1 H), 8.57 (d, $J=5.7$ Hz, 1 H). HRMS (ESI) $[M+H]^+$, Calcd for $C_{34}H_{29}F_4IrN_3O_4$ 812.1712, found 812.1718. Anal. Calcd for $C_{34}H_{28}F_4IrN_3O_4$: C, 50.36; H, 3.48; N, 5.18. Found: C, 48.39; H, 3.86; N, 4.71.

3. Results and discussion

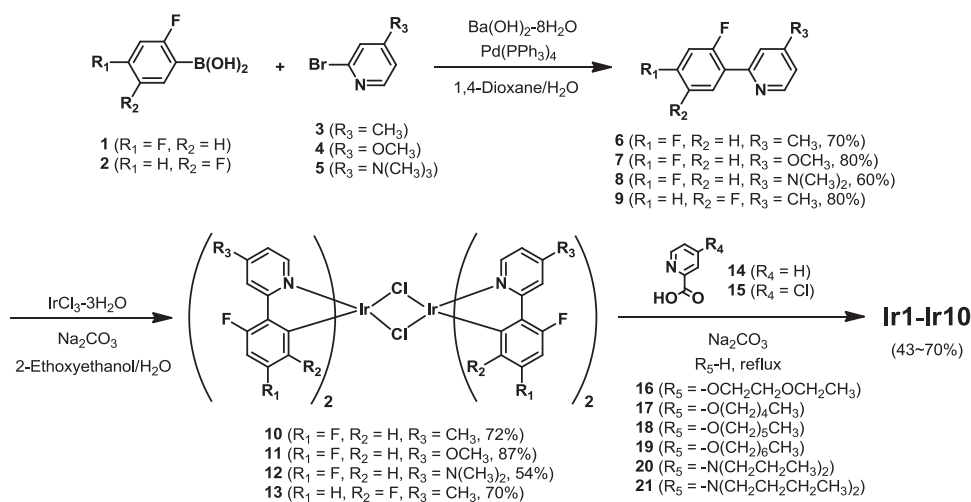
3.1. Synthesis of iridium(III) complexes, Ir1–Ir10

We prepared four different 2-phenylpyridine derivatives as main ligands. Methyl, methoxy or dimethylamino group was introduced as an electron donating group on the C-4 of the pyridine ring of the main ligand. Two fluoro groups as electron withdrawing groups were substituted on the 2-, 4- or 2-, 5-position of the phenyl ring of the main ligand. Picolinates substituted at their 4-positions with various alkoxy- or dialkylamino group as potent electron donating groups were used as ancillary ligands of iridium(III) complexes. The substituted 2-phenylpyridines, **6–9**, employed as the main ligands in the new iridium (III) complexes, were synthesized using the well-known Suzuki palladium-catalyzed cross coupling reaction between substituted-phenylboronic acids (**1** or **2**) and substituted-2-bromopyridines (**3**, **4** or **5**) as shown in [Scheme 1](#). These pyridine derivatives were transformed to the corresponding μ -chloro-bridged iridium dimers, **10–13** using the method described by Nonoyama [34]. The heteroleptic iridium(III) complex, **Ir1**, was reported earlier [35], and prepared by refluxing μ -chloro-bridged iridium dimer **10** and chloropicolinic acid in the presence of sodium carbonate in ethoxyethanol. Other heteroleptic iridium(III) complexes, **Ir2–Ir10**, were prepared by treating each of μ -chloro-bridged iridium dimers, **10–13**, with 4-chloropicolinic acid in nucleophilic solvent such as highly boiling alcohols (**16–19**) and amines (**20**, **21**) at the elevated temperature in the presence of sodium carbonate. Successful generations of the μ -chloro-bridged iridium dimers **10–13** could be confirmed by elemental analysis although NMR data were not actively utilized for the confirmation due to their low solubility in organic NMR solvents.

3.2. Single-crystal structural analysis of Ir2, Ir3, and Ir4

For X-ray structural analysis, single crystals of selected iridium complexes, **Ir2**, **Ir3** and **Ir4**, were generated by crystallization from chloroform/hexane at room temperature. X-ray crystallographic data of these complexes show that they all have heteroleptic meridional rather than facial configurations. ORTEP plots of the crystallographic data for **Ir2**, **Ir3**, and **Ir4** are shown in [Fig. 3](#) and the data, refinement, and selected geometrical parameters are given in [Tables S1 and S2](#).

All carbon-carbon (C–C) and carbon-nitrogen (C–N) bond lengths and angles in the structures of the heteroleptic iridium(III) complexes were typical for substances containing N-heteroaromatic and aromatic ring systems and similar to the values reported previously for $(C^N)_2Ir(acac)$ [31]. The Ir–C bond between the metal and main ligand in complex **Ir2** (Ir–C₁₂ = 1.980(7) Å) was shorter than that of the Ir–N bond (Ir–N₁ = 2.015(5) Å) and similar to the Ir–C bond lengths of 1.980(7)–1.982(7) Å reported for (ppy)₂Ir(acac) and (tpy)₂Ir(acac) complexes. The longer Ir–C₂₇ bond (Ir–C₂₇ = 1.991(4) Å > Ir–C₁₂ = 1.970(4) Å) in **Ir3**, Ir–C₈ bond (Ir–C₈ = 2.010(8) Å > Ir–C₂₃ = 1.973(7) Å) in **Ir4** appeared to be a consequence of the trans influence of the ancillary ligand.



Scheme 1. Synthesis of heteroleptic Iridium(III) complexes, Ir1-Ir10.

3.3. Photophysical properties

Absorption and emission spectra of synthesized iridium(III) complexes **Ir1-Ir10** were measured in ethanol solution and are displayed in Figs. S2–S11. Their maximum absorption and emission wavelengths along with emission quantum efficiencies in solution and film states are given in Table 1.

Ir1, Ir2, Ir4, and Ir7 exhibit absorption bands that correspond to $^1\text{LC}^*(^1\pi-\pi^*)$ of 230–300 nm, $^1\text{MLCT}^*(^1\text{d}-\pi^*)$ of 350–400 nm, and weak but detectable $^3\text{MLCT}^*(^3\text{d}-\pi^*)$ transitions of 420–450 nm (Fig. 4(a)). In contrast, the absorption spectrum of sole main ligand which is lack of iridium metal does not contain bands corresponding to these transitions (Fig. S1).

Ir1 shows broad emission maximum at 512 nm and emission shoulder at bluer region of 464 nm in ethanol solution with full half-width maximum (FWHM) of 106 nm (Fig. 4(b)). In chloroform solution, however, **Ir1** exhibits emission maximum at 464 nm and second emission at 512 nm in reverse manner [35]. Both **Ir2** and **Ir4**, which have 2'-(ethoxy)ethoxy and hexyloxy group on the C-4 of picolinate, respectively, are observed to show almost identical emission spectra with the emission maximum at 464 nm. Substitution of the dibutylamino group on the C-4 of picolinate in **Ir7** lead to 2 nm bathochromic shifted emission maximum at 466 nm compared to that of **Ir2** and **Ir4**. In addition, introducing the long-alkoxy, (2'-(ethoxy)ethoxy and hexyloxy) and bulky dibutyl amino group on the C-4 of picolinate ancillary ligand (**Ir2, Ir4** and **Ir7**) are found to increase the relative emission intensity around at 464–466 nm, but decrease the emission peak intensity around at 500 nm. Furthermore **Ir2, Ir4** and **Ir7** show narrower FWHM range of emission (57–64 nm) than that of **Ir1**. Interestingly, **Ir2, Ir4** or **Ir7** containing a long chain or bulky substituents on the C-4 of picolinate ancillary ligand showed 1.3–1.7 times higher emission quantum efficiency (Φ_p) in solution state than

Table 1

Characteristics of the UV–vis absorption and photoluminescence data of heteroleptic iridium(III) complexes Ir1-Ir10 at 298 K. ^aMaximum emission wavelength.

Iridium complexes	Solution ^a			Film		
	Abs _{max} (nm)	PL _{max} (nm)	Φ_{PL}^b	Abs _{max} (nm)	PL _{max} (nm)	Φ_{PL}^c
Ir1	255, 372	464, 512 [*]	0.44	262, 382	515	0.11
Ir2	251, 365	464 [*] , 490	0.69	263, 380	467 [*] , 493	0.20
Ir3	256, 376	464 [*] , 490	0.77	263, 380	468 [*] , 490	0.23
Ir4	256, 376	464 [*] , 489	0.77	263, 380	468 [*] , 490	0.28
Ir5	256, 376	464 [*] , 490	0.77	263, 380	467 [*] , 490	0.21
Ir6	266, 377	466 [*] , 492	0.57	279, 382	473 [*] , 492	0.20
Ir7	266, 377	466 [*] , 492	0.57	279, 382	472 [*] , 492	0.21
Ir8	253, 362	464, 490 [*]	0.14	267, 380	467, 492	0.03
Ir9	259, 365	533	0.08	270, 380	534	0.01
Ir10	247, 386	470 [*] , 499	0.47	262, 391	477, 503	0.11

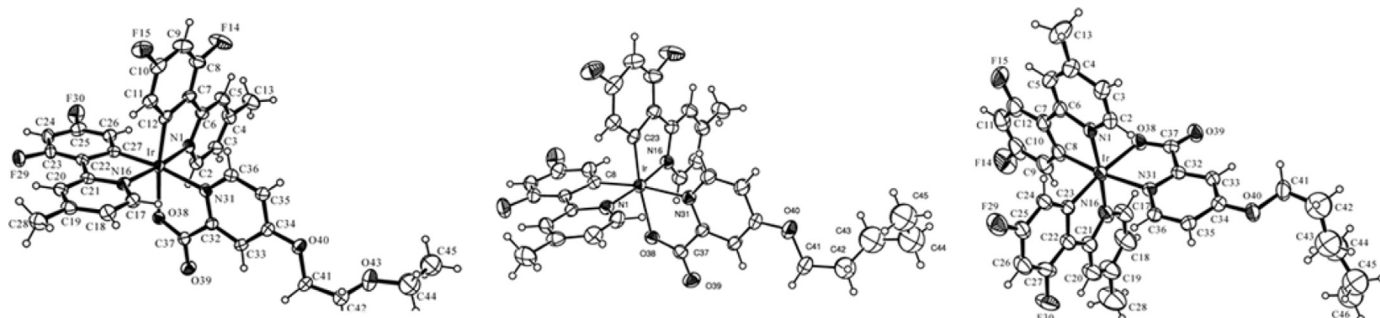
^a The emission spectra were obtained in degassed ethanol at 298 K (1.5×10^{-5} M).

^b The quantum yield (Φ_{PL}) of solution condition was measured in degassed ethanol solution at 298 K with the use of Ir(ppy)₂acac ($\Phi_{\text{PL}} = 0.34$) [36] as a standard.

^c The quantum yield (Φ_{PL}) of film condition was measured using 9,10-diphenylanthracene as standard ($\Phi_{\text{PL}} = 0.83$) [31]. Films were prepared by spin coating from chloroform.

that of **Ir1**. Additionally, **Ir2, Ir4, and Ir7** exhibited 1.8–2.5 times higher Φ_p even in film state than that of **Ir1**. The relatively long distance which could be present between neighboring iridium(III) complexes containing long-alkoxy or bulky dibutyl amino substituent on the ancillary ligand seems to decrease the phosphorescence quenching and, consequently, enhance the Φ_p .

Ir4 and **Ir5** show the absorption spectrum arising from $^1\text{LC}^*(^1\pi-\pi^*)$ at 256 nm, $^1\text{MLCT}^*(^1\text{d}-\pi^*)$ at 376 nm, and $^3\text{MLCT}^*(^3\text{d}-\pi^*)$ transition at 453 nm (Fig. 5(a)). In emission spectrum, here as elsewhere, they show

Fig. 3. ORTEP diagram of heteroleptic iridium(III) complexes **Ir2** (left), **Ir3** (center) and **Ir4** (right). The thermal ellipsoids for the image represent 30% probability limit.

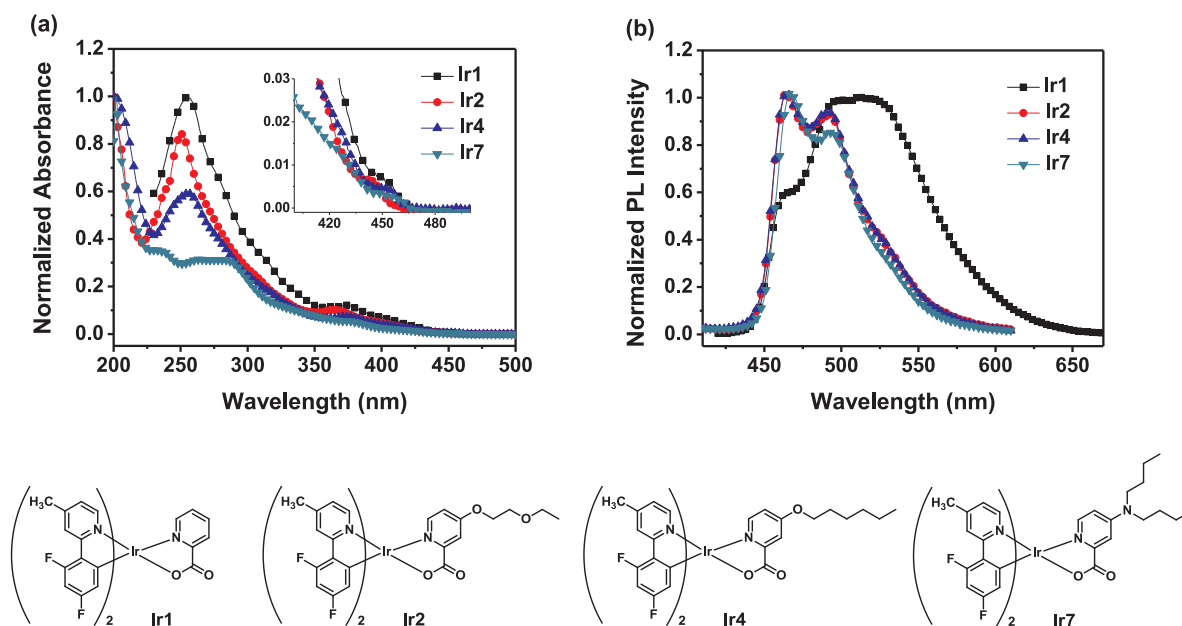


Fig. 4. (a) UV-vis absorption and (b) emission spectra of heteroleptic iridium(III) complexes of **Ir1**, **Ir2**, **Ir4**, and **Ir7** in ethanol solutions.

same emission maximum at 464 nm with $\Phi_p = 0.77$ irrespective of chain length of hexyloxy or heptyloxy on the C-4 position of picolinate (Fig. 5(b)).

Interestingly, electron donating methyl, methoxy, and dimethylamino substituents on the C-4 position of the pyridine ring of 2-phenylpyridine main ligand significantly affect the emission wavelength. **Ir2** and **Ir8** have similar absorption spectrum in solution state (Fig. 6(a)). **Ir2** containing a methyl substituent on the C-4 position of the pyridine ring of the main ligand exhibit the absorption bands of $^1LC^*(^1\pi-\pi^*)$ at 251 nm, $^1MLCT^*(^1d-\pi^*)$ at 365 nm, and $^3MLCT^*(^3d-\pi^*)$ transition at 453 nm. **Ir8** containing a methoxy substituent exhibit the absorption bands of $^1LC^*(^1\pi-\pi^*)$ at 253 nm and $^1MLCT^*(^1d-\pi^*)$ at 362 nm similarly with **Ir2**, but very weak $^3MLCT^*(^3d-\pi^*)$ transition at 450 nm. **Ir9** containing a dimethylamino substituent on the C-4 position of the pyridine ring of the main ligand show a more resolved absorption spectrum than that of **Ir2** or **Ir8**. In addition to the absorption peaks

corresponding to $^1LC^*(^1\pi-\pi^*)$ at 259 nm and $^1MLCT^*(^1d-\pi^*)$ at 365 nm, an additional absorption peak at 307 nm between $^1LC^*$ and $^1MLCT^*$ transition is observed in the absorption spectrum of **Ir9**. Unlike the other iridium(III) complexes, **Ir9** shows weakest $^3MLCT^*$ transition and consequently imply lowest emission quantum efficiency by the weak spin-orbit coupling among the synthesized iridium(III) complexes.

Ir2 has the emission maximum at 464 nm and the second emission peak at 490 nm as shown in Fig. 6(b). In the case of **Ir8** emission intensity at 464 nm becomes decreased, but 490 nm is increased relatively with an emission shoulder at 520 nm (Fig. 6(b)). In addition, the emission spectrum of **Ir8** lying between those of **Ir2** and **Ir9** is found to be broader (FWHM = 101 nm) than that of **Ir2** (FWHM = 61 nm). **Ir8** shows a lower phosphorescence efficiency (Φ_p) of 0.14 than that ($\Phi_p = 0.44$) of **Ir2**. Surprisingly **Ir9** exhibits broad and structureless emission with maximum at 533 nm (FWHM = 84 nm) and shows larger Stokes shift than **Ir2** and **Ir8**. The strong electron donating dimethyla-

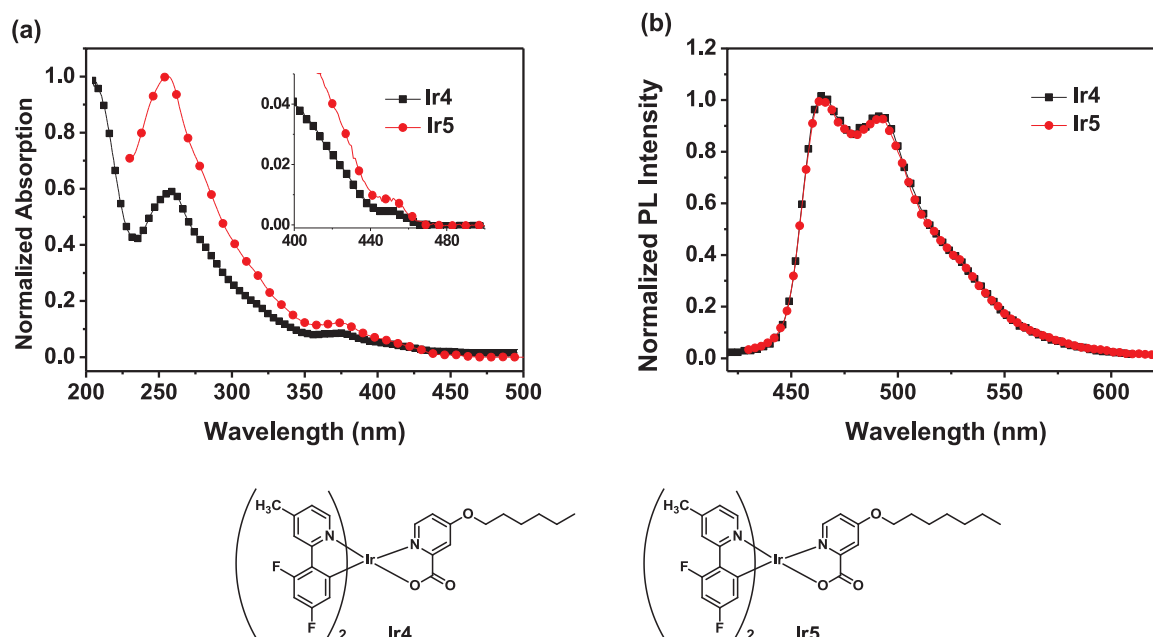


Fig. 5. (a) UV-vis absorption and (b) emission spectra of heteroleptic iridium(III) complexes, **Ir4** and **Ir5** in ethanol solutions.

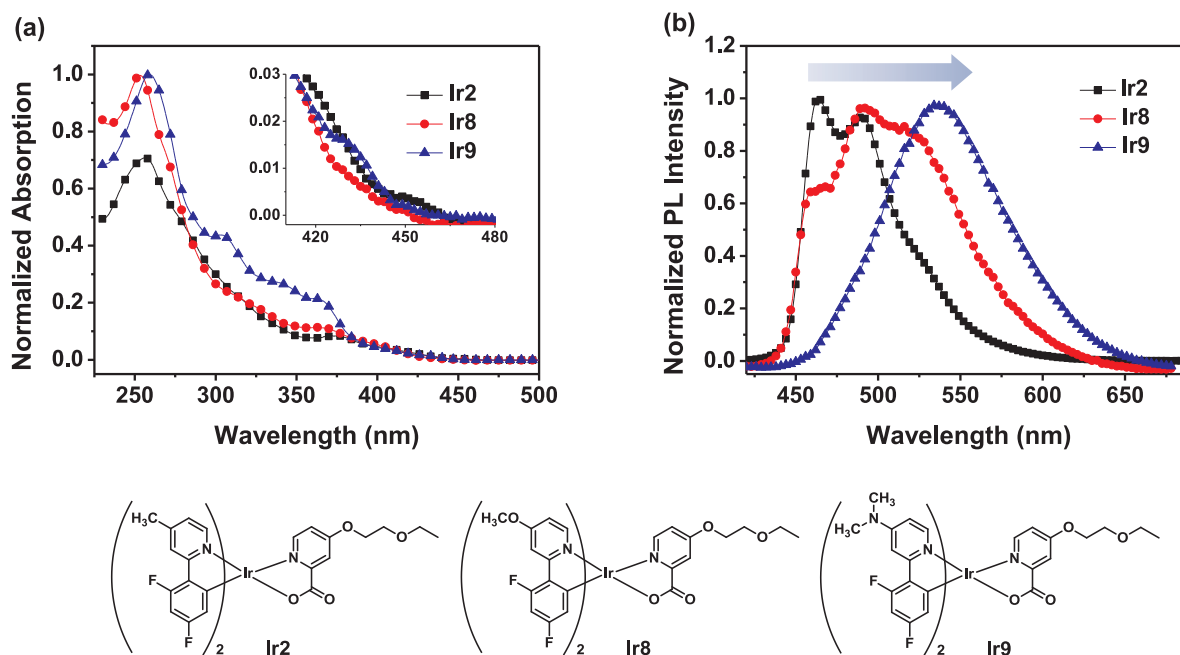


Fig. 6. (a) UV-vis absorption and (b) emission spectra of heteroleptic iridium(III) complexes of **Ir2**, **Ir8**, and **Ir9** in ethanol solutions.

mino substituent on the C-4 position of the pyridin ring of the main ligand of **Ir9** leads to the bathochromic shift of the emission maximum by 69 nm compared to the emission maximum of **Ir2** ($\lambda_{\text{max}} = 464$ nm). This observation can not be explained by simple electron donating effect on the HOMO and LUMO distribution. Furthermore, **Ir9** is found to show much lower phosphorescence efficiency (Φ_p) of 0.08 than that ($\Phi_p = 0.44$) of **Ir2**.

Contrary to our expectation, the electron donating ability of the substituent on the C-4 position of the pyridin ring of the main ligand increases as $-\text{CH}_3 < -\text{OCH}_3 < -\text{N}(\text{CH}_3)_2$, the HOMO-LUMO energy band gap decreases, leading bathochromic shift rather than hypsochromic shift in emission. The similar absorption spectra of **Ir2**, **Ir8** and **Ir9** indicate that they have similar $S_0 \rightarrow S_1$ transition energy while the emission spectrum of **Ir9** shows that its emitting triplet state (T_1) energy is lower than that of **Ir2** and **Ir8**. Decreased T_1 state energy increases the energy difference between S_1 and T_1 and, consequently, decreases the intersystem crossing (ISC) rate and phosphorescence efficiency of **Ir9**. The emission of **Ir9** seems to occur via the energy transfer from ${}^3\text{MLCT}^*$ to the triplet state of ligand judging from the emission maximum [37].

Ir10 which is composed with 2-(2',5'-difluorophenyl)-4-methylpyridine as a main ligand exhibits the emission maximum at 470 nm with $\Phi_p = 0.47$. Changing the position of the electron withdrawing fluorine substituent from 4'-position to 5'-position of the phenyl ring of the main ligand leads to bathochromic shift in emission by 6 nm compared with that of **Ir2** as we predicted (Fig. S11).

3.4. DFT calculations on the iridium(III) complexes

As pointed out above, there was a significant difference between the experimentally determined emission properties of the heteroleptic iridium(III) complexes and those expected based on the initial predictions. In particular, the substitution of a methyl group with a more strongly electron-donating methoxy or dialkylamino group at the C-4 position of the pyridine ring of the main ligand in the complex results in a significant bathochromic rather than a hypsochromic shift of the phosphorescence emission maxima. For example, **Ir2** and **Ir7**, both of which contain a methyl group at the C-4 position of the pyridine ring of the main ligand, but possess picolinate C-4 alkoxy and dialkylamino group, respectively, have a corresponding emission wavelength max-

imum at 464 and 466 nm. In contrast, **Ir9** containing a more strongly electron-donating dimethylamino group at the C-4 position of the pyridine ring of the main ligand and a picolinate C-4 alkoxy group has an emission maximum at 531 nm.

To better understand the experimentally observed photophysical properties of phosphorescent iridium complexes and to uncover the source of the discrepancy pointed out above, density functional theory (DFT) calculations were performed on **Ir1-Ir3** and **Ir7-Ir10** employing the Becke's three parameterized Lee-Yang-Parr (B3LYP) exchange correlation functional using a suite of Gaussian 09 programs [38]. The Hay-Wadt effective core potential (ECP) of double zeta basis set (LANL2DZ) was used for iridium and the 6-311+G** basis sets were used for the other atoms. This level of theory has been applied successfully to similar systems in previous studies [39–41]. The ligands in all complexes were considered to be coordinated to the iridium metal with octahedral geometry. No significant structural changes were found in these complexes despite the variation of ligands.

The calculated HOMO-LUMO energy gaps ($E_{\text{H-L}}$) for **Ir1-Ir3** and **Ir7-Ir10** are shown in Fig. S12 and Table S3 and highest occupied (HOMOs) and the lowest unoccupied (LUMOs) molecular orbitals of **Ir2**, **Ir8**, and **Ir9** are shown in Fig. 7. For all complexes, the electrons in the HOMOs are distributed mainly over the iridium metal and the main ligands, but the electron distributions of LUMOs differ from complex to complex. In **Ir2** and **Ir8**, the LUMOs are distributed over both the main and ancillary ligands while it is relatively localized at the central regions of the ancillary ligand for **Ir9**. Consequently, it might be concluded from an analysis of the frontier orbital distributions that the complexes undergo both metal to ligand charge transfer (MLCT) as well as $\pi\text{-}\pi^*$ transitions (inter-ligand energy transfer; ILET) in a manner dependent on the electronic nature and position of the substituents.

3.5. OLED device fabrication

Among **Ir2-Ir5** and **Ir7**, highly phosphorescent **Ir7** was selected to fabricate OLED as a dopant material. Electrochemical and thermal stabilities of the synthesized blue phosphorescent iridium(III) complexes were investigated (Figs. S13 and S14 and Tables S4 and S5) and **Ir7** showed the best thermal stability up to 357 °C among them. **Ir2** was also used as a dopant in the emissive layer to compare the performances of fabricated devices. OLEDs were fabricated on clean glass substrates

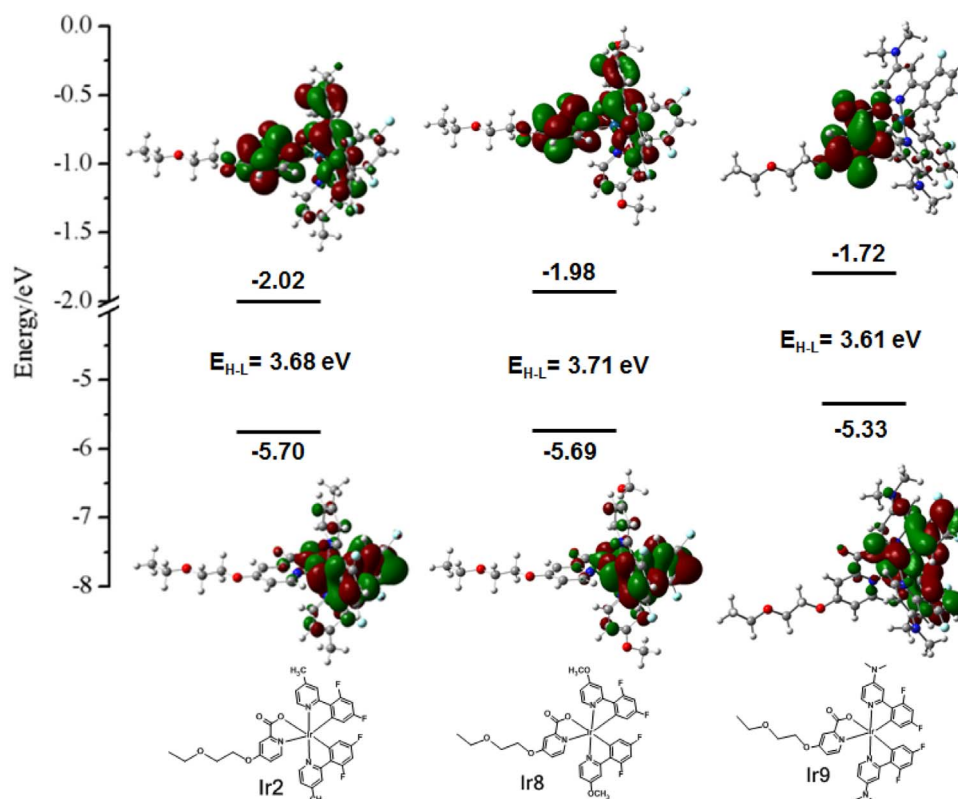


Fig. 7. Calculated HOMO and LUMO of Ir2, Ir8, and Ir9 obtained from DFT calculations.

precoated with indium tin oxide (ITO) by thermal evaporation under vacuum. Prior to the deposition of the organic layer, the ITO substrates were degreased with acetone and IPA followed by exposure to a UV-ozone flux for 10 min. All organic layers were deposited sequentially on ITO coated substrates, employing thermal evaporation at a base pressure of $< 5 \times 10^{-8}$ Torr, in the following order: hole transporting layer (HTL)/emitting layer (EML)/hole blocking layer (HBL)/electron transporting layer (ETL)/cathode. HTL was a 30-nm-thick NPB (*N,N'*-bis-(1-naphthyl)-*N,N'*-diphenyl-1,1'-biphenyl-4,4'-diamine). Each EML consisted of a 30 nm thick mCP (*N,N'*-dicarbazolyl-3,5-benzene) layer doped with 6 wt% of the iridium complex, Ir2 or Ir7. The HBL is a 10 nm thick BCP (2,9-dimethyl-4,7-diphenyl-1,10-phenanthroline) and the ETL was a 40 nm thick Alq₃ [42].

The EL spectra of OLEDs constructed using Ir2 and Ir7 were observed to display a wavelength maximum at 465 and 470 nm, respectively. The performance characteristics of the devices are summarized in Table 2. The current density-voltage (*I-V*) and luminescence-voltage (*L-V*) characteristics of the devices with the configuration are given in Fig. 8(a) and (b). The turn-on voltages of the devices containing Ir2 and Ir7 are 7–7.5 V and their respective maximum luminescence are 2900 and 6000 cd/m² at 13 V. The external quantum efficiencies as a function of the luminance of OLEDs using 6 wt% complexes Ir2 and Ir7 as the emitting layer are shown Fig. 8(c). The maximum EQE of

complex Ir2 was observed at a current density of ca. 1 mA/cm², but it decreased at higher current densities. On the other hand, the EQE of complex Ir7 increase continuously up to a current density of 40 mA/cm².

4. Conclusion

New heteroleptic iridium(III) complexes containing alkoxy or *N,N*-dialkyl amino groups at the 4-position of the picolinate ancillary ligand were synthesized readily and efficiently by reacting cyclometalated μ -chloro-bridged iridium(III) dimers with 4-chloropicolinic acid in the presence of sodium carbonate in a high boiling nucleophilic solvent, such as 2-ethoxyethanol, pentanol, hexanol, heptanol, dibutylamine, or dipropylamine. During the process of producing the iridium(III) complexes, the 4-chloro group of 4-chloropicolinic acid was substituted by the nucleophilic solvent. Substitution of a long-alkoxy or *N,N*-dialkylamino group on the C-4 position of picolinate of the ancillary ligand brought to the improvement of phosphorescence quantum efficiency (Φ_p). Ir2–Ir7 showed 1.3–1.8 times higher Φ_p in solution state and 1.8–2.5 times higher Φ_p in film state than that of Ir1 which has methyl on the C-4 position of picolinate. Different chain length on the C-4 position of picolinate of Ir2–Ir5 had no impact on the emission maximum wavelength exhibited at 464 nm ($\Phi_p = 0.69$ –0.77). Introduction of an electron donating group on the C-4 position of the pyridine ring of the main ligand undergoes substantial changes on the emission wavelength. Against our expectation, increasing the electron donating ability along with $-\text{CH}_3 < -\text{OCH}_3 < -\text{N}(\text{CH}_3)_2$ caused bathochromic shift in emission maximum rather than hypsochromic shift. Two distinguishable emission peaks were observed in Ir2, which were attributed to the emission originated from both the main and ancillary ligands, while Ir9 showed only one broad emission maxima presumably through ILET. It might be concluded from analysis of the photophysical properties and the frontier orbital distributions that the complexes undergo both of the metal to ligand charge transfer (MLCT) and π - π^* transition (ILET) in a manner dependent on the electronic nature and

Table 2

Performance characteristics of OLED devices constructed using Ir2 and Ir7.

Complexes	Turn-on voltage ^a (V)	Current density ^b (mA/cm ²)	Luminance ^b (cd/M ²)	EQE _{max} ^c (%)	CIE (x,y)
Ir2	7.5	120	2900	2.7	0.18, 0.30
Ir7	7	194	6000	1.7	–

^a Voltage required to reach at 1 mA/cm².

^b Measured under the condition of brightness at 13 V.

^c Maximum external quantum efficiency.

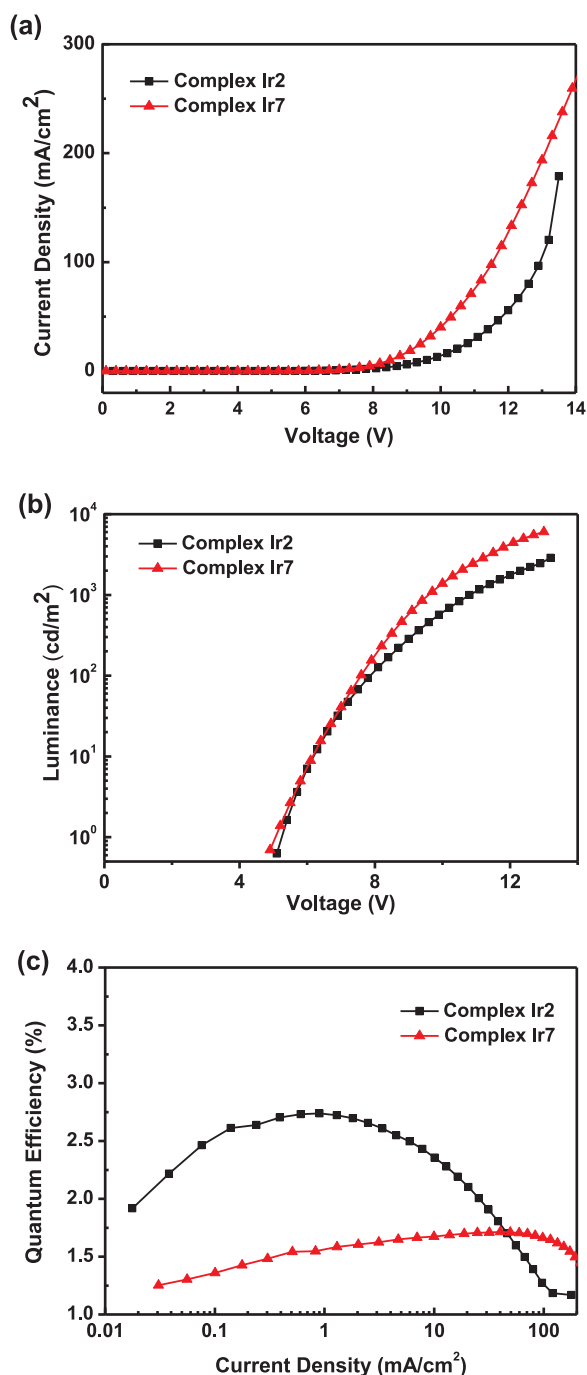


Fig. 8. (a) Current density-voltage (*I*-*V*) and (b) luminescence-voltage (*L*-*V*) characteristics of the devices fabricated from Ir2 and Ir7 with the configuration of ITO/NPB/mCP:iridium complex/BCP/Alq₃/LiF/Al. (c) External quantum efficiencies of OLEDs as a function of luminance using 6 wt% complexes Ir2 and Ir7 as the emitting layer, respectively.

position of the substituents. In addition to providing potentially useful blue emitting dopants for OLED studies, this effort would provide valuable informations for designing main and ancillary ligands for color tuning with substituents of heteroleptic iridium(III) complexes.

Acknowledgements

This study was supported by Basic Science Research Program through the National Research Foundation of Korea (NRF) funded by the Ministry of Education, Science and Technology (NRF-2013R1A6A3A03020498 for H. J. Park) and Solvay, SA. (Brussel,

Belgium). The device test was done at the OLED Center of Seoul National University (Professor Jang-Joo Kim) and the helpful consultation and advice from Professor Sung Ho Jin are acknowledged.

Appendix A. Supplementary material

Supplementary data associated with this article can be found in the online version at <http://dx.doi.org/10.1016/j.jlum.2017.04.043>.

References

- [1] C.W. Tan, S.A. Vanslyke, *Appl. Phys. Lett.* 51 (1987) 913.
- [2] R.H. Friend, R.W. Gymer, A.B. Holmes, J.H. Burroughes, R.N. Marks, C. Taliani, D.C. Bradley, D.A. Dos Santos, J.L. Brédas, M. Lögdlund, W.R. Salaneck, *Nature* 397 (1999) 121.
- [3] L.S. Hung, C.H. Chen, *Mater. Sci. Eng.* 39 (2002) 143.
- [4] M.K. Nazeeruddin, R. Dumphy-Baker, D. Berner, S. River, L. Zuppiroli, M. Graetzel, *J. Am. Chem. Soc.* 125 (2003) 8790.
- [5] W.-Y. Wong, C.-L. Ho, *J. Mater. Chem.* 19 (2009) 4457.
- [6] W.-Y. Wong, C.-L. Ho, *Coord. Chem. Rev.* 253 (2009) 1709.
- [7] G. Zhou, W.-Y. Wong, S. Suoc, *J. Photochem. Photobiol. C: Photochem. Rev.* 11 (2010) 133.
- [8] G. Zhou, W.-Y. Wong, X. Yang, *Chem. Asian J.* 6 (2011) 1706.
- [9] H.J. Park, J.N. Kim, H.-J. Yoo, K.-R. Wee, S.O. Kang, D.W. Cho, U.C. Yoon, *J. Org. Chem.* 78 (2013) 8054.
- [10] C.-L. Ho, W.-Y. Wong, *New J. Chem.* 37 (2013) 1665.
- [11] L. Ying, C.-L. Ho, H. Wu, Y. Cao, W.-Y. Wong, *Adv. Mater.* 26 (2014) 2459.
- [12] X. Yang, G. Zhou, W.-Y. Wong, *J. Mater. Chem. C* 2 (2014) 1760.
- [13] X. Xu, X. Yang, J. Zhao, G. Zhou, W.-Y. Wong, *Asian J. Org. Chem.* 4 (2015) 394.
- [14] X. Yang, G. Zhou, W.-Y. Wong, *Chem. Soc. Rev.* 44 (2015) 8484.
- [15] C. Yao, J. Li, J. Wang, X. Xu, R. Liu, L. Li, *J. Mater. Chem. C* 3 (2015) 8675.
- [16] J. Lee, H.-F. Chen, T. Batagoda, C. Coburn, P.I. Djurovich, M.E. Thompson, S.R. Forrest, *Nat. Mater.* 15 (2016) 92.
- [17] J.H. Kim, M.S. Liu, A.K.Y. Jen, B. Carlson, L.R. Dalton, D.F. Shu, R. Dodda, *Appl. Phys. Lett.* 83 (2003) 776.
- [18] H. Wu, G. Zhou, J. Zou, C.-L. Ho, W.-Y. Wong, W. Yang, J. Peng, Y. Cao, *Adv. Mater.* 21 (2009) 4181.
- [19] J. Zou, H. Wu, C.-S. Lam, C. Wang, J. Zhu, C. Zhong, S. Hu, C.-L. Ho, G.-J. Zhou, H. Wu, W.C.H. Choy, J. Peng, Y. Cao, W.-Y. Wong, *Adv. Mater.* 23 (2011) 2976.
- [20] B. Zhang, G. Tan, C.-S. Lam, B. Yao, C.-L. Ho, L. Liu, Z. Xie, W.-Y. Wong, J. Ding, L. Wang, *Adv. Mater.* 24 (2012) 1873.
- [21] K.-H. Kim, C.-K. Moon, J.-H. Lee, S.-Y. Kim, J.-J. Kim, *Adv. Mater.* 26 (2014) 3844.
- [22] T.-L. Chiu, H.-J. Chen, Y.-H. Hsieh, J.-J. Huang, M.-K. Leung, *J. Phys. Chem. C* 119 (2015) 16846.
- [23] K.-H. Kim, S.-Y. Park, *Org. Electron.* 36 (2016) 103.
- [24] S. Wu, S. Li, Q. Sun, C. Huang, M.-K. Fung, *Sci. Rep.* 6 (2016) 25821.
- [25] S. Stolz, M. Petzoldt, S. Dueck, M. Sendner, U.H.F. Bunz, U. Lemmer, M. Hamberger, G. Hernandez-Sosa, *ACS Appl. Mater. Interfaces* 8 (2016) 12959.
- [26] H. Shin, J.-H. Lee, C.-K. Moon, J.-S. Huh, B. Sim, J.-J. Kim, *Adv. Mater.* 28 (2016) 4920.
- [27] M.J. Jurov, C. Mayr, T.D. Schmidt, T. Lampe, P.I. Djurovich, W. Brütting, M.E. Thompson, *Nat. Mater.* 15 (2016) 85.
- [28] P.J. Hay, *J. Phys. Chem. A* 106 (2002) 1634.
- [29] S.-C. Lo, C.P. Shipley, R.G. Berra, R.E. Harding, A.R. Cowley, P.L. Burn, I.D.W. Samuel, *Chem. Mater.* 18 (2006) 5119.
- [30] S. Lamansky, P. Djurovich, D. Murphy, F. Abdel-Razzaq, H.E. Lee, C. Adachi, P.E. Burrows, S.R. Forrest, M.E. Thompson, *J. Am. Chem. Soc.* 123 (2001) 4304.
- [31] C. Adachi, R.C. Kwong, P. Djurovich, V. Adamovich, M.A. Baldo, M.E. Thompson, S.R. Forrest, *Appl. Phys. Lett.* 79 (2001) 2082.
- [32] J. Brooks, Y. Babayan, S. Lamansky, P.I. Djurovich, I. Tsyba, R. Bau, M.E. Thompson, *Inorg. Chem.* 41 (2002) 3055.
- [33] S.H. Jin, O.S. Jung, Y.I. Kim, M.H. Hyun, J.W. Lee, U.C. Yoon, M.K. Nazeeruddin, C. Klein, M. Graetzel, *Light-Emitting Material*, PCT Int. Appl. WO 2007042474, 2007.
- [34] M. Nonoyama, *Bull. Chem. Soc. Jpn.* 47 (1974) 767.
- [35] W. Cho, G. Sarada, J.-S. Park, Y.-S. Gal, J.H. Lee, S.-H. Jin, *Org. Electron.* 15 (2014) 2328.
- [36] M.A. Baldo, S. Lamansky, P.E. Burrows, M.E. Thompson, S.R. Forrest, *Appl. Phys. Lett.* 75 (1999) 4.
- [37] H.J. Lee, Y. Ha, *Polym. Bull.* 73 (2016) 2501.
- [38] M.J. Frisch, G.W. Trucks, H.B. Schlegel, G.E. Scuseria, M.A. Robb, et al., *Gaussian 09*, revision A.1; Gaussian, Inc., Wallingford CT, 2009.
- [39] S. Kang, J.Y. Lee, S.H. Jung, H.S. Kim, M.Y. Chae, S.H. Jin, *Adv. Funct. Mater.* 19 (2009) 2205.
- [40] S.J. Lee, J.S. Park, K.J. Yoon, Y.I. Kim, S.H. Jin, S.K. Kang, Y.S. Gal, S. Kang, J.Y. Lee, J.W. Kang, S.H. Lee, H.D. Park, J.J. Kim, *Adv. Funct. Mater.* 18 (2008) 3922.
- [41] M. Song, J.S. Park, Y.S. Gal, S. Kang, J.Y. Lee, J.W. Lee, S.H. Jin, *J. Phys. Chem. C* 116 (2012) 7526.
- [42] J.W. Kang, D.S. Lee, H.D. Park, J.W. Kim, W.I. Jeong, Y.S. Park, S.H. Lee, K. Go, J.S. Lee, J.J. Kim, *Org. Electron.* 9 (2008) 452.